Construction and Building Materials 200 (2019) 630–636

Contents lists available at ScienceDirect

Construction and Building Materials

journal homepage: www.elsevier.com/locate/conbuildmat

Technical note

A computational framework for quantifying reactivity of fly ash in cement pastes from backscattered electron images

S.M. Park [a], Beomjoo Yang [b], Haemin Jeon [c,*]

[a] Department of Civil and Environmental Engineering, Korea Advanced Institute of Science and Technology (KAIST), 291 Daehak-ro, Yuseong-gu, Daejeon 34141, Republic of Korea
[b] School of Civil Engineering, Chungbuk National University, Chungdae-ro 1, Seowon-Gu, Cheongju, Chungbuk 28644, Republic of Korea
[c] Department of Civil and Environmental Engineering, Hanbat National University, 125 Dongseo-daero, Yuseong-gu, Daejeon 34158, Republic of Korea

ARTICLE INFO

Article history:
Received 24 August 2018
Received in revised form 7 December 2018
Accepted 21 December 2018

Keywords:
Fly ash
Image analysis
SEM/BSE
Geopolymer

ABSTRACT

A computational framework for quantifying reactivity of fly ash in cement pastes from backscattered electron images is proposed. Alkali-activated fly ash samples were synthesized, and were used for acquiring backscattered electron images at various ages. The obtained images were processed by a computational tool, which employs image binarization using adaptive threshold, and region-of-interest-based objective contour. The proposed scheme offered means of quantifying various information from images such as volume of cracks/voids, unreacted particles, and binder matrix. The degree of reaction of fly ash in alkali-activated fly ash samples at various ages was calculated and compared with that obtained by selective dissolution experiments. The result shows that the proposed computational scheme can be used for quantifying the reactivity of fly ash in cement pastes.

© 2018 Elsevier Ltd. All rights reserved.

1. Introduction

Low-calcium fly ash, an industrial by-product of coal power plants, is a widely appreciated construction material, which can be used as a partial or full replacement of ordinary Portland cement (PC) as blended PC or as geopolymer, respectively [1,2]. Use of fly ash in a partial replacement of PC is effective to enhance the durability performance of concrete against aggressive actions such as fire [3,4], alkali-aggregate reaction [5], and acid attack [6]. The hydraulic reactivity of fly ash is much lower than that of PC, hence it often requires chemical activation (high pH) in order to initiate their reaction [7]. This condition is achieved by provision of an alkali-activator in geopolymer leading to formation of aluminosilicate gel from fly ash, and high pH pore solution in blended PC which induces pozzolanic reaction with portlandite [8,9].

Despite a vast number of relevant studies conducted thus far, no single standardized protocol is available for measurement of fly ash reactivity in a hardened cementitious matrix. From the materials science perspective, fly ash reactivity is one of the primary parameters required for thermodynamic modelling [10], hence, has been an important topic of numerous studies in the relevant research community [11]. Techniques for quantifying the reactivity of fly ash can be categorized into indirect and direct methods on a broad scale. The degree of reaction of fly ash in blended PC can be indirectly determined using techniques such as calorimetry, thermogravimetry, and measuring chemical shrinkage [7,11]. While these indirect methods are efficient in terms of sample preparation and qualitative comparison purposes, the obtained results may not always correlate with the actual reactivity of fly ash. These techniques require use of an inert reference material, although even inert materials can induce filler effect accelerating hydration, hence violating its primary role as a reference [7,12]. In addition, one should be cautious with employing thermogravimetry for quantifying reactivity of fly ash, since quantifying consumption of portlandite in fly ash blended PC samples is difficult due to dehydration-induced weight loss and gives a lower value of fly ash reactivity in comparison with other direct methods [11].

Direct methods, on the other hand, concern with techniques which directly probe unreacted fly ash (or reaction product) in a binder matrix. Each technique can be advantageous over others or have its own weakness, so it is advised to treat values and trends obtained by each technique separately. For instance, selective dissolution technique using acid (i.e., salicylic acid, hydrochloric acid, etc.) can be as accurate as dissolving almost 0 wt% raw fly ash [11], while some hydrates may persist even after dissolution treatment [13]. ^{29}Si magic-angle-spinning (MAS) nuclear magnetic resonance (NMR) spectroscopy, as often used to quantify reaction degree of cement (specifically tri- and di-calcium silicate) [14,15], is difficult

* Corresponding author.
E-mail address: hjeon@hanbat.ac.kr (H. Jeon).

https://doi.org/10.1016/j.conbuildmat.2018.12.160
0950-0618/© 2018 Elsevier Ltd. All rights reserved.

to be adopted for fly ash due to the presence of Fe [7]. In addition, X-ray diffraction with Rietveld refinement and coupled with Partial Or No Known Crystal Structure (PONKCS) method can be a useful technique to observe the reaction kinetic of fly ash in blended PC. This method is based on intensity-based procedure which employs a crystal structure (or phases for modelling various amorphous phases) with unknown lattice parameters [16,17]. For instance, the amorphous hump due to the glass of raw fly ash in X-ray diffraction patterns can be modelled by introducing a tetragonal structure (i.e., with the following cell parameters a = b, and alpha = beta = gamma = 90°). A significant amount of work is being conducted to standardize this technique against other techniques in order to provide accurate quantification of X-ray amorphous phases along with other crystalline phases. Nevertheless, the RILEM round robin test on degree of reaction of slag and fly ash in blended cements concluded that the degree of reaction determination based on PONKCS has less precision in comparison with other techniques studied (selective dissolution, SEM-image analysis, thermogravimetry, etc.) while this technique requires an adoption of an accurate model for amorphous phases (phases with unknown lattice parameters such as calcium-silicate-hydrate) and the quality of obtained results highly depends on the expertise of the analyst [11].

In the present study, analysis of images acquired from scanning electron microscope (SEM) in a backscattered electron (BSE) mode is deemed suitable to derive sufficiently good quality of reactivity data and other useful quantitative information from polished and coated samples such as porosity [18], pore structure [19], anhydrous cement [20] and other supplementary cementitious materials [7,11]. A computational tool is proven to be an effective means of conducting such image analyses as evidenced by a study [7] proposing an computational scheme for obtaining fly ash reactivity information from BSE images, and by allowing quantification of reactivity of high calcium fly ash, which is often difficult with other techniques [21], by coupling with elemental mapping results. Quantification methods based on image analysis on one hand allows acquisition of results with sufficiently good quality, while numerous drawbacks yet remain unsolved. For instance, some fly ash particles show similar grey level as reaction products, which makes separation and identification of unreacted particles from reaction products [11]. Specifically, accurate identification of unreacted fly ash is mandatory in order to minimize the error associated with such image analyses. The present study therefore proposes an adaptive detection algorithm for identifying unreacted fly ash from an SEM image using various image processing techniques such as the image binarization using adaptive threshold, object detection by measuring properties of blobbed image regions.

2. Experimental and analytical procedure

The chemical composition of the fly ash obtained by means of X-ray fluorescence is shown in Table 1. The X-ray diffraction pattern (obtained using an X'Pert APD, PHILIPS, at KBSI Daegu Center, South Korea) of the fly ash shown in Fig. 1 presented crystalline phases of quartz, mullite, and some iron oxide which are typically observed in fly ash, along with an amorphous hump centered at 25° 2θ. The particle size distribution of the fly ash measured by laser diffraction is shown in Fig. 2. The fly ash was activated by a 9 M NaOH solution at a Na_2O dosage of 10.3 g per 100 g of fly ash.

All samples were synthesized with a liquid-to-solid ratio of 0.5. For synthesis of samples, the fly ash and the activating solution were mixed using a hand mixer for 5 min at room temperature. The fresh alkali-activated fly ash paste was poured into a vial, and was cured in a chamber at 80 °C for the initial 24 h. Note that the initial curing of samples at an elevated temperature was to induce fly ash reaction which requires a higher activation energy than other room-temperature-cured binders [22]. The samples were either sealed in a plastic bag or exposed to an elevated CO_2 level of 10% to reduce the reaction kinetic [23] by carbonating the alkalis and neutralizing the pore solution which hinders remaining raw fly ash to react [24]. These conditions were

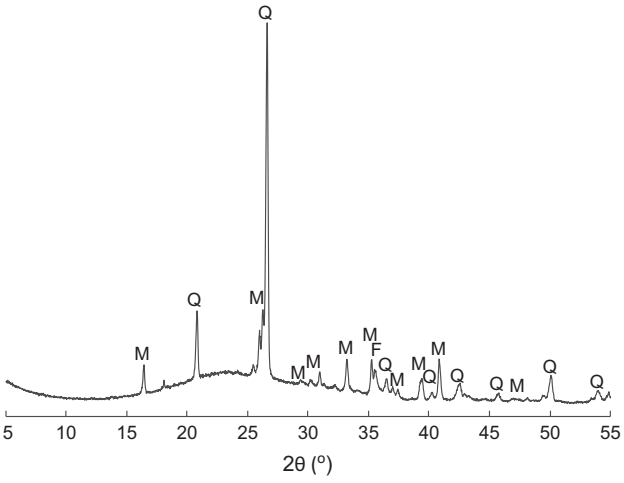

Fig. 1. X-ray diffraction pattern of the raw fly ash. The following annotations were used to denote: Q – quartz (SiO_2, PDF# 01-085-1054), M – mullite ($3Al_2O_3{\cdot}2SiO_2$, PDF# 00-006-0258), and F – iron oxide (Fe_2O_3, PDF# 01-073-0603).

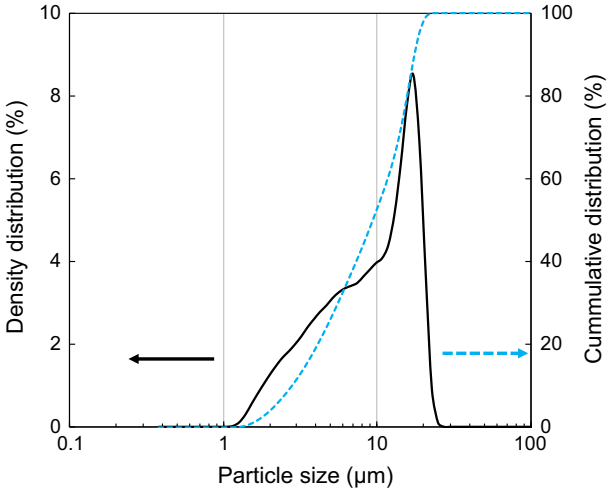

Fig. 2. Particle size distribution of the raw fly ash.

Table 1
Chemical composition of the fly ash used in this study.

(wt%)	SiO_2	Al_2O_3	Fe_2O_3	CaO	MgO	P_2O_5	TiO_2	K_2O	SO_3	LOI*
Fly ash	57.0	21.0	10.0	4.8	1.3	1.5	1.5	1.4	1.0	2.7

* Loss on ignition.

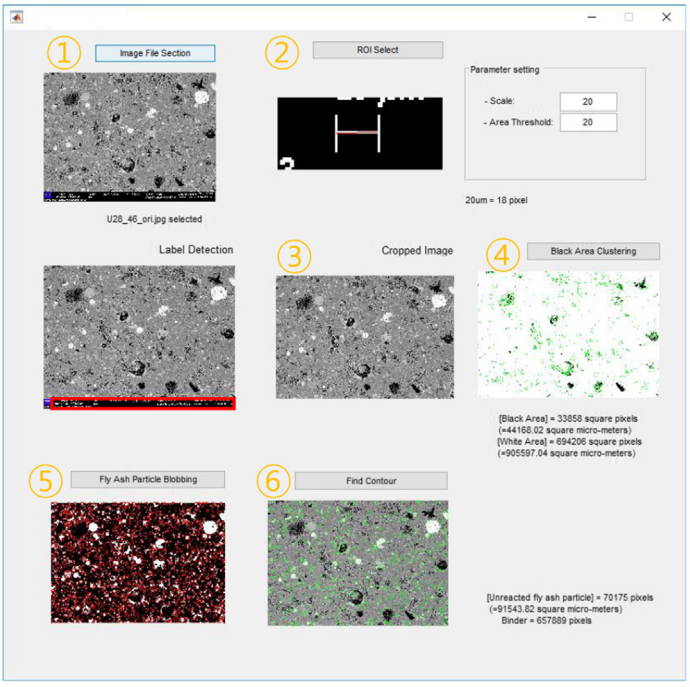

(a)

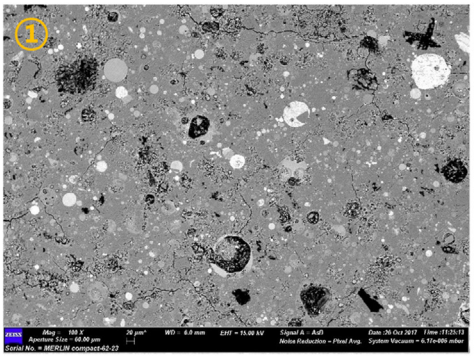

(b)

(c)

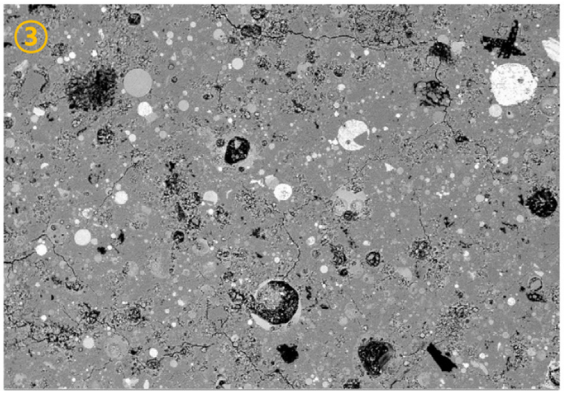

(d)

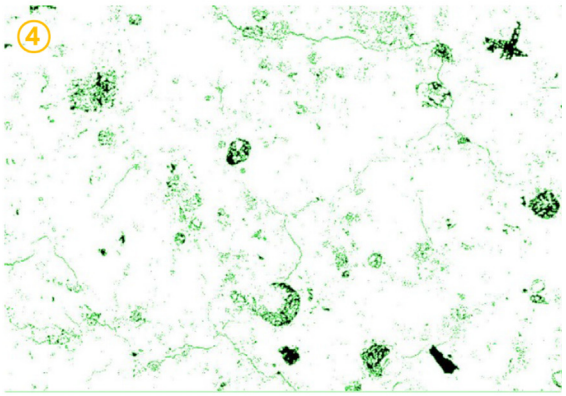

(e)

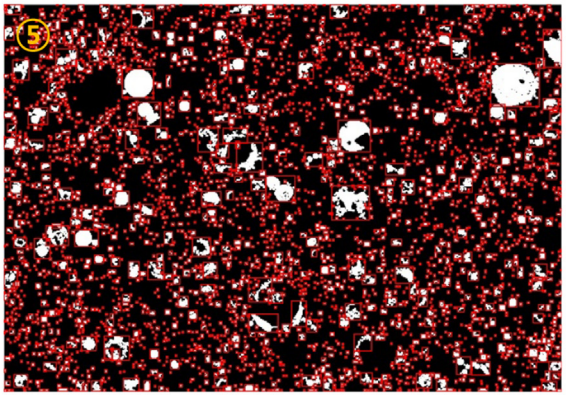

(f)

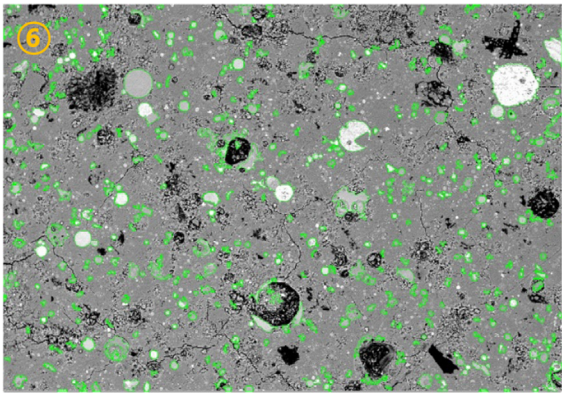

(g)

Fig. 3. Analysis procedure for quantifying reaction degree of fly ash: (a) GUI of the developed in-house software, (b) original SEM image, (c) selecting and defining the scale bar, (d) the image to be analyzed after cropping the SEM labels, (e) identifying non-solid part, (f) converting into a binary image and blobbing ROI, (g) final identification of unreacted fly ash particles.

provided for 28 days, thereafter the samples were immersed in isopropanol and were slowly evaporated under vacuum for 72 h to arrest further reaction by solvent exchange and avoid damage associated with rapid drying [25]. Another set of samples was immersed in isopropanol immediately after the 24 h of initial curing.

The samples were impregnated with a low-viscosity epoxy after drying the solvent from the samples. The impregnated samples were dry-polished using SiC with a grit number of 400, 800, 1200, 2000, and 4000. These samples were then coated with osmium before being loaded on the sample stage for SEM analysis. SEM images were taken using Low Voltage Field Emission Scanning Electron Microscope (Merlin Compact) at various magnifications in vacuum conditions at 15 keV. The reactivity of the fly ash was measured by selective dissolution method, dissolving ~1 g of the paste sample in a 1:20 HCl, as described in [16,26].

A graphic user interface based on MATLAB, which employs image binarization using adaptive threshold, and region-of-interest (ROI)-based objective contour, is developed to quantify the reactivity of fly ash in a cementitious material by detecting unreacted fly ash in an SEM image (Fig. 3(a)). First, an original SEM image taken using a polished sample of alkali-activated fly ash is loaded into the program (Fig. 3(b)). The digital image length scale is converted to take into account of the real scale, i.e., converting pixels into micrometers, using the scale bar provided in the image (Fig. 3(c)). An area threshold can be enabled to offset the analysis of certain particles with size below the set threshold (Fig. 3(c)). Then, the label section at the bottom of the image showing SEM experimental details is removed (Fig. 3(d)). Before detecting unreacted fly ash particles from the image, non-solid part throughout the binder matrix (i.e., cracks, and voids) is quantified (Fig. 3(e)). The area corresponding to non-solid is deducted from the total area of the image, hence, considering the solid binder matrix only. This is done by converting the original 3-channel color image into a 1-channel gray image, as shown in Fig. 4(a) and (b). The gray image is then converted into a binary image consisting of black and white (Fig. 4(c)), by employing the method by Otsu [27] for automatically setting the threshold level for gray-level histograms which is used in the image conversion. The image is converted into a binary image to detect bright regions, which denote unreacted fly ash particles (Fig. 3(f)). These areas are blobbed and selected as an ROI, and particles with the greatest size in each

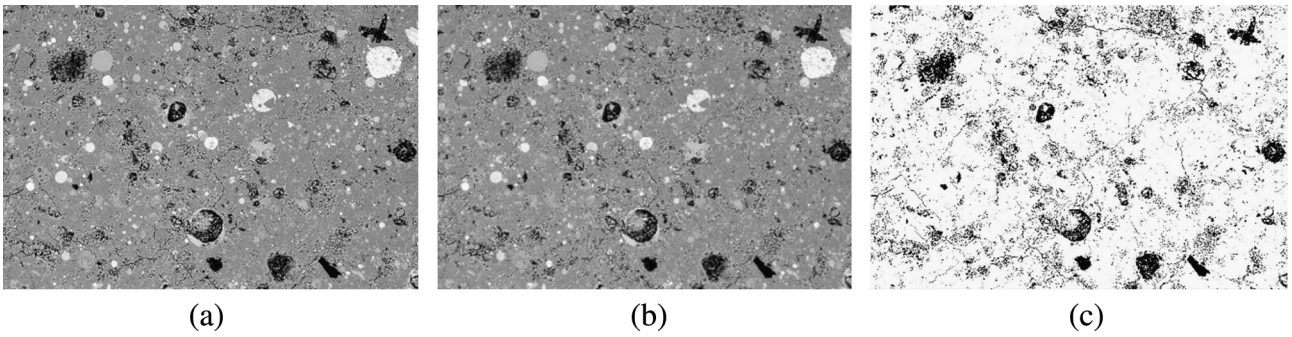

Fig. 4. Detailed procedure for detecting non-solid parts from images. (a) 3-channel original image, (b) 1-channel gray image, and (c) binary image used for identifying non-solid parts.

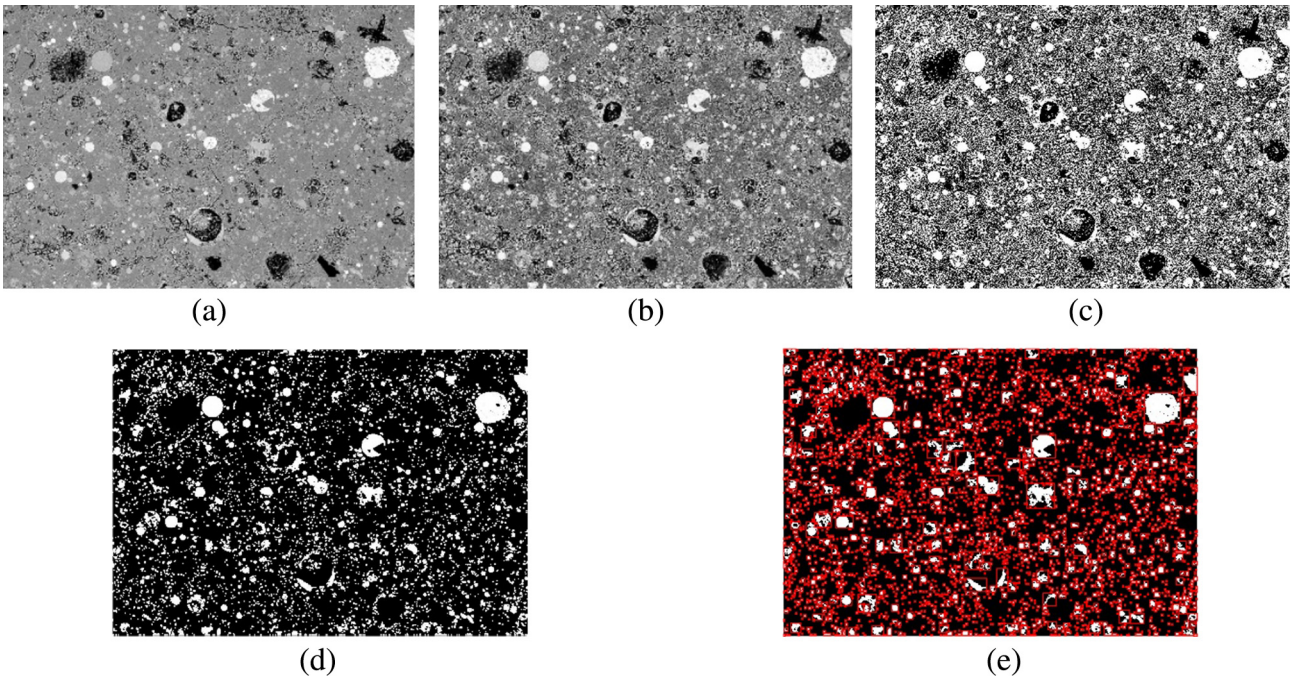

Fig. 5. Detailed procedure for detecting unreacted fly ash. (a) 1-channel gray image, (b) equalized image, (c) binary image, (d) image after morphology operation, and (e) blobbing conducted in the image obtained in (d).

blob are contoured, as shown in Fig. 3(g). This procedure is shown in detail in Fig. 5. Firstly, the original image is converted into a 1-channel gray image, as identical to the process described for obtaining the image in Fig. 4(b). This image undergoes contrast-limited adaptive histogram equalization to obtain the image in Fig. 5(b), and thereafter setting up the threshold for gray-level histograms and creating a binary image in Fig. 5(c). Finally, morphology operation is done on the image by undergoing degradation and expansion (Fig. 5(d)), to eliminate noises and allow accurate blobbing as shown in Fig. 5(e).

3. Results and discussion

Typical images obtained from the computational analysis are shown in Fig. 6. It is noted, particularly in Fig. 6(c), that cracks and voids are adequately separated from the binder matrix by the proposed analytical scheme. Unlike reactivity estimation based on mass measurement (i.e., selective dissolution) which is free from effect of non-solid present in the binder matrix, it is important to estimate and separate the air content [7]. The volume of air void was considered by measuring the volume fraction of a paste sample in a previous study [7], while the proposed scheme offers means of estimating the void observed in each image. This procedure, on one hand, is found useful to identify cracks and interfacial transition zone between a binder matrix and an unreacted particle, while distinction with dark particles (Fe-rich fly ash particles) is difficult (Fig. 6(a)).

The reactivity of fly ash was calculated by computing the amount of unreacted fly ash presented on the image taken at various magnifications, and is summarized in Fig. 7. The result generally indicated an increase in the reactivity as a function of time, as expected due to the prolonged reaction of fly ash. The reactivity calculated from images taken at magnifications of 1000 and 2000 were similar regardless of the sample age, while that at 100 magnification showed a larger value. The fly ash used in this study had a medium particle size of 10.8 μm, and hence, the lowest magnification (i.e., 100) may not have been well-suited for the purpose of visualizing small particles.

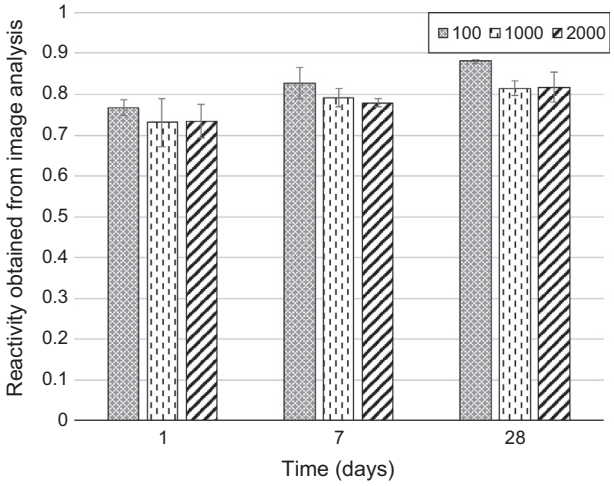

Fig. 7. Reactivity of fly ash calculated from analyzing images at various magnifications.

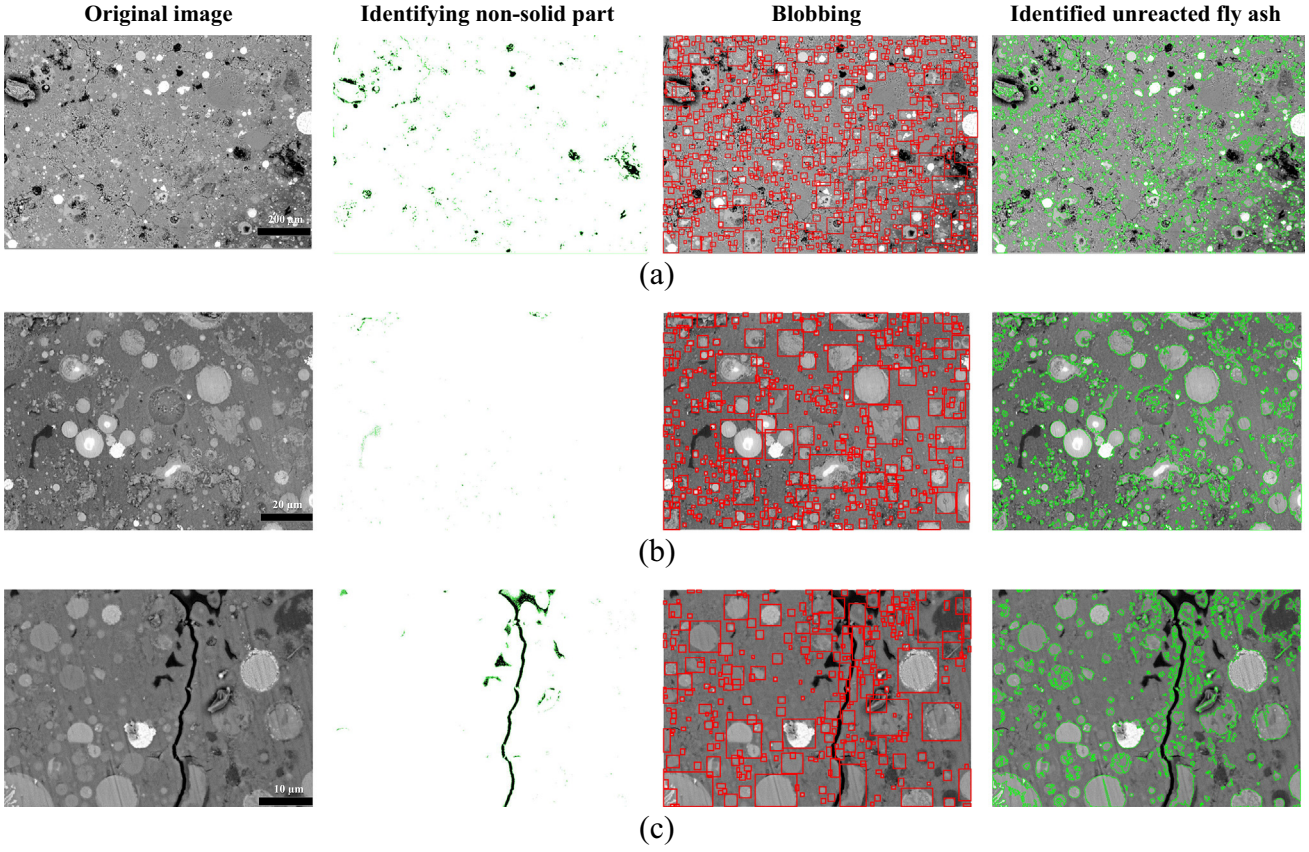

Fig. 6. Typical images obtained by the analysis. Images were taken at (a) 100, (b) 1000, and (c) 2000 magnifications. Red rectangles in the third column are blobbed areas in the image, which are taken for identification of unreacted fly ash as indicated by green solid lines in the fourth column. (For interpretation of the references to colour in this figure legend, the reader is referred to the web version of this article.)

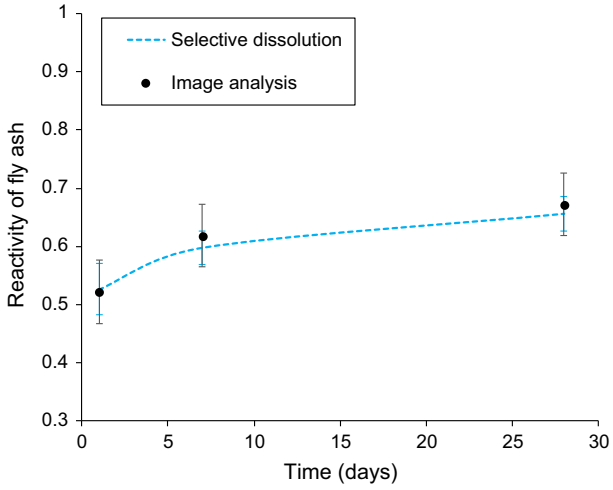

Fig. 8. Reactivity of fly ash calculated from analyzing images at various magnifications. Error bars indicate one standard deviation from either side of the mean values obtained in the selective dissolution and image analysis.

It is noted that the proposed scheme generally overestimates the reactivity of fly ash in geopolymer, in comparison to those observed by dissolution experiments conducted at similar sample ages (cf. [16,26]), while the reactivity of fly ash calculated from SEM image analysis is reported to give an overestimated value, thus requires a correction for systematic error, as expressed in Eq. (1) [7].

$$\textit{Corrected reactivity} = 1 - \frac{f_{FA}}{1-e} \tag{1}$$

where f_{FA} is fraction of unreacted fly ash, and e is the systematic error of the image analysis. The origin of the error can be due to the missing identification during the image analysis, but can also be related to instrumental errors [7,13,21]. Note that this calculation assumes that the error associated with the reactivity measurement by selective dissolution is negligible. Moreover, since the reactivity calculated from the 2-D image analysis cannot take into account of dissolution of spherical-shaped fly ash particles, errors associated with volumetric information inevitably occur. Hence, the systematic error described here also contains that associated with translating 3-D information into 2-D images.

The corrected reactivity is compared with the reactivity measured by selective dissolution in Fig. 8. The value of e was adjusted as 0.44 so that the reactivity at 1 day obtained from the image analysis matches that obtained by the selective dissolution, then assuming a constant reaction kinetic that point onward. This was done by referring to previous studies of quantifying reactivity of fly ash blended in Portland cement, which often assume that the reactivity of the fly ash obtained by the analysis at an early age when no fly ash is expected to have reacted is used to zero-set [7]. The result shows that the reactivity corrected after obtaining from the image analysis is in a close proximate to that obtained by dissolution technique, suggesting viability of the image analysis technique for quantifying the degree of reaction of fly ash in cementitious materials.

4. Conclusions and perspectives

The present study proposed a computational framework for quantifying the degree of reaction of fly ash in cement pastes from BSE images. This scheme identifies the non-solid part of the binder matrix from a BSE image, hence excluding cracks and voids and only considering the binder matrix during the image analysis. After correcting the error typically associated with image analysis techniques, the final degree of reaction of fly ash was in a close proximate with that obtained experimentally.

Nevertheless, since the material dealt in this study is insulating, such SEM images can suffer from charging. The reaction degree estimated from images suffering from charging was found to be overestimated, while this can be prevented by appropriate sample preparation (i.e., coating) [28]. Due to the nature of image analysis, a choice of appropriate resolution is mandatory. It is suggested that the images for quantifying reaction degree (especially of fly ash) or similar purposes are taken at a magnification of at least 1000. Note that using images with higher resolution (i.e., taking images at higher magnifications) can be computationally expensive since it will increase the size of blobs and time taken for analysis of each blob. It is believed that a more accurate quantification can be employed by calibrating against samples with known information (degree of reaction, porosity, phase compositions), considering the true density of binder gel that thus far remains unknown, and correcting the 2-D image analysis results to take into account of spherical shape of fly ash particles with known particle diameters. This technique can be further extended by integrating with other image analysis techniques (i.e., image segmentation), which may then give other detailed information, for instance, the size of the particles remaining after reaction.

Conflict of interest

None.

References

[1] P. Duxson, A. Fernández-Jiménez, J.L. Provis, G.C. Lukey, A. Palomo, J. Van Deventer, Geopolymer technology: the current state of the art, J. Mater. Sci. 42 (9) (2007) 2917–2933.
[2] E. Gartner, Industrially interesting approaches to "low-CO_2" cements, Cem. Concr. Res. 34 (9) (2004) 1489–1498.
[3] S. Donatello, C. Kuenzel, A. Palomo, A. Fernández-Jiménez, High temperature resistance of a very high volume fly ash cement paste, Cem. Concr. Compos. 45 (2014) 234–242.
[4] S.M. Park, J.G. Jang, N.K. Lee, H.K. Lee, Physicochemical properties of binder gel in alkali-activated fly ash/slag exposed to high temperatures, Cem. Concr. Res. 89 (2016) 72–79.
[5] H. Chen, J. Soles, V. Malhotra, Investigations of supplementary cementing materials for reducing alkali-aggregate reactions, Cem. Concr. Compos. 15 (1–2) (1993) 75–84.
[6] K. Torii, M. Kawamura, Effects of fly ash and silica fume on the resistance of mortar to sulfuric acid and sulfate attack, Cem. Concr. Res. 24 (2) (1994) 361–370.
[7] F. Deschner, B. Münch, F. Winnefeld, B. Lothenbach, Quantification of fly ash in hydrated, blended Portland cement pastes by backscattered electron imaging, J. Microsc. 251 (2) (2013) 188–204.
[8] A. Fraay, J. Bijen, Y. De Haan, The reaction of fly ash in concrete a critical examination, Cem. Concr. Res. 19 (2) (1989) 235–246.
[9] H.F. Taylor, Cement Chemistry, Thomas Telford, 1997.
[10] K. De Weerdt, M.B. Haha, G. Le Saout, K.O. Kjellsen, H. Justnes, B. Lothenbach, Hydration mechanisms of ternary Portland cements containing limestone powder and fly ash, Cem. Concr. Res. 41 (3) (2011) 279–291.
[11] P.T. Durdziński, M.B. Haha, S.A. Bernal, N. De Belie, E. Gruyaert, B. Lothenbach, E.M. Méndez, J.L. Provis, A. Schöler, C. Stabler, Outcomes of the RILEM round robin on degree of reaction of slag and fly ash in blended cements, Mater. Struct. 50 (2) (2017) 135.
[12] R. Snellings, G. Mertens, J. Elsen, Supplementary cementitious materials, Rev. Mineral. Geochem. 74 (1) (2012) 211–278.
[13] M.B. Haha, K. De Weerdt, B. Lothenbach, Quantification of the degree of reaction of fly ash, Cem. Concr. Res. 40 (11) (2010) 1620–1629.
[14] J. Hjorth, J. Skibsted, H. Jakobsen, ^{29}Si MAS NMR studies of Portland cement components and effects of microsilica on the hydration reaction, Cem. Concr. Res. 18 (5) (1988) 789–798.
[15] C.M. Dobson, D.G. Goberdhan, J.D. Ramsay, S.A. Rodger, ^{29}Si MAS NMR study of the hydration of tricalcium silicate in the presence of finely divided silica, J. Mater. Sci. 23 (11) (1988) 4108–4114.
[16] G.B. Singh, K.V. Subramaniam, Quantitative XRD study of amorphous phase in alkali activated low calcium siliceous fly ash, Constr. Build. Mater. 124 (2016) 139–147.
[17] R. Snellings, A. Salze, K. Scrivener, Use of X-ray diffraction to quantify amorphous supplementary cementitious materials in anhydrous and hydrated blended cements, Cem. Concr. Res. 64 (2014) 89–98.

[18] H. Zhao, D. Darwin, Quantitative backscattered electron analysis of cement paste, Cem. Concr. Res. 22 (4) (1992) 695–706.
[19] Y. Wang, S. Diamond, An approach to quantitative image analysis for cement pastes, MRS Online Proc. Lib. Arch. 370 (1994).
[20] K.L. Scrivener, H. Patel, P. Pratt, L. Parrott, Analysis of phases in cement paste using backscattered electron images, methanol adsorption and thermogravimetric analysis, MRS Online Proc. Lib. Arch. 85 (1986).
[21] P.T. Durdziński, C.F. Dunant, M.B. Haha, K.L. Scrivener, A new quantification method based on SEM-EDS to assess fly ash composition and study the reaction of its individual components in hydrating cement paste, Cem. Concr. Res. 73 (2015) 111–122.
[22] Z. Sun, A. Vollpracht, Isothermal calorimetry and in-situ XRD study of the NaOH activated fly ash, metakaolin and slag, Cem. Concr. Res. 103 (2018) 110–122.
[23] S. Park, J. Jang, G. Kim, H. Lee, Strength development of alkali-activated fly ash exposed to a carbon dioxide-rich environment at an early age, J. Korean Ceram. Soc. 53 (1) (2016) 18–23.
[24] S.A. Bernal, J.L. Provis, B. Walkley, R. San Nicolas, J.D. Gehman, D.G. Brice, A.R. Kilcullen, P. Duxson, J.S. van Deventer, Gel nanostructure in alkali-activated binders based on slag and fly ash, and effects of accelerated carbonation, Cem. Concr. Res. 53 (2013) 127–144.
[25] I. Ismail, S.A. Bernal, J.L. Provis, R. San Nicolas, D.G. Brice, A.R. Kilcullen, S. Hamdan, J.S. van Deventer, Influence of fly ash on the water and chloride permeability of alkali-activated slag mortars and concretes, Constr. Build. Mater. 48 (2013) 1187–1201.
[26] M. Criado, A. Fernández-Jiménez, A. De La Torre, M. Aranda, A. Palomo, An XRD study of the effect of the SiO_2/Na_2O ratio on the alkali activation of fly ash, Cem. Concr. Res. 37 (5) (2007) 671–679.
[27] N. Otsu, A threshold selection method from gray-level histograms, IEEE Trans. Syst. Man Cybern. 9 (1) (1979) 62–66.
[28] K. Chung, J. Reisner, E. Campbell, Charging phenomena in the scanning electron microscopy of conductor-insulator composites: a tool for composite structural analysis, J. Appl. Phys. 54 (11) (1983) 6099–6112.